Phys. Status Solidi A **206**, No. 7, 1520–1524 (2009) / **DOI** 10.1002/pssa.200824402

physica status solidi a
www.pss-a.com
applications and materials science

Highly stable re-dispersibility of nanocrystalline TiO_2 observed during anatase–rutile phase transformation

Yanting Li[1], Xiuguo Sun[1], Huiwan Li[2], and Yu Wei[*,2]

[1] School of Materials Science and Engineering, Shijiazhuang Railway Institute, 050043 Shijiazhuang, P.R. China
[2] College of Chemistry and Material Science, Hebei Normal University, 050016 Shijiazhuang, P.R. China

Received 25 September 2008, revised 21 March 2009, accepted 8 April 2009
Published online 26 May 2009

PACS 64.70.Nd, 65.80.+n, 68.08.De, 68.43.–h, 81.07.Bc

[*] Corresponding author: e-mail weiyu@mail.hebtu.edu.cn, Phone: +86 311 8626 8342, Fax: +86 311 8589 3425

TiO_2 nanoparticles were prepared employing forced hydrolysis of titanium tetrachloride in an acid aqueous solution. We observed the highly stable dispersibility of TiO_2 nanoparticles calcined at 600 °C and 700 °C in water. X-ray diffraction (XRD) showed that the phase transformation from anatase (A) to rutile (R) occurred when the nanoparticles were calcined over 600 °C. Transmission electron microscope (TEM), Fourier-transform infrared spectroscopy (FT-IR) and Thermo-gravimetric analysis (TGA) showed that the phase transformation led to the formation of the better spherical particlesis, which were in favour of water adsorption onto the surface of the TiO_2. The Brunauer–Emmett–Teller (BET) data of particles calcined at different temperatures showed that the surface hydration forces impeded TiO_2 particles aggregation and resulted in the high structural stability during A–R phases transformation. Zeta potentials of TiO_2 nanoparticles calcined at different temperature showed the electrostatic forces were not crucial factors in the stable dispersibility. A model illustrated that the spherical particles of TiO_2 allowed maintaining the high density of water on the surface of TiO_2 nanoparticles.

© 2009 WILEY-VCH Verlag GmbH & Co. KGaA, Weinheim

1 Introduction Nanosized TiO_2 has attracted increasing attention in the scientific community for its wide applications in photocatalysts [1, 2], solar cells [3], gas sensors [4] and optoelectronic devices [5]. The applications of TiO_2 are primarily determined by its physicochemical properties such as crystallite structure, particle size, specific surface area, porosity and thermal stability [6–10].

TiO_2 usually exists in the form of anatase (A), rutile (R) and brookite (brookite is a minority product of most synthesis). In photocatalytic study, anatase TiO_2 is generally considered to be more active than rutile crystalline [11]. Moreover, anatase TiO_2 with high crystallinity is preferred for photocatalysis, since high crystallinity would mean few defects for the recombination of photogenerated electrons and holes [12]. Hence, calcination is a common treatment that can be used to increase the photocatalytic activities [13]. Some attentions are also focused on the composite of two phases of TiO_2, which has a much higher photocatalytic activity than pure anatase or rutile TiO_2 nanoparticles [14, 15]. Especially, Bakardjieva et al. [16] reported that the significantly enhanced photocatalytical activity had been observed in the region of the A–R transformation. However, the detailed mechanism and factors influencing its photocatalytical activity are poorly understood [17–19]. Furthermore, severe aggregation has taken place in the process of preparation, subsequent treatment and application because of its small particle size and large specific surfaces. Thus, investigating the relationship between the dispersibility of TiO_2 nanoparticles and the phase transformation becomes one of the key issues in achieving higher photocatalytic activity and understanding the catalytic behaviors of the TiO_2 (especially for mixture of A and R).

Herein, TiO_2 nanoparticles were prepared employing forced hydrolysis of titanium tetrachloride ($TiCl_4$) in an acid aqueous solution at boiling reflux. The obtained products were calcined in an oven at different temperatures. Then, the dispersibility of TiO_2 nanoparticles in water me-

WILEY InterScience® DISCOVER SOMETHING GREAT

© 2009 WILEY-VCH Verlag GmbH & Co. KGaA, Weinheim

dium was studied by the sedimentation method. It was found that TiO_2 nanoparticles, which were during phase transformation from A to R, had the highly stable dispersibility. We showed evidences suggesting that the phase transformation is in favor of the adsorption of water onto the surface of TiO_2 nanoparticles. The repulsive surface hydration force, which was considered to be stronger than electrostatic forces between TiO_2 nanoparticles, prevented the nanoparticles from aggregating.

2 Experimental

2.1 Preparation of TiO_2 nanoparticles A portion of $TiCl_4$ was added dropwise into 250 ml of ice-water under vigorous stirring and controlled the final concentration of $TiCl_4$ was 0.4 mol l^{-1}. Then the concentrated H_2SO_4 was added to the solution and controlled the final concentration of H_2SO_4 was 0.3 mol l^{-1}. The mixture solution was heated to boiling reflux under severely stirring, and the heating rate was controlled to be 10–15 °C min^{-1}. After reacting for 5 h, the white precipitates were filtered and washed repeatedly with water, until the Cl^- ions in the precipitates were completely removed, and dried at 50 °C for 24 h in a vacuum oven.

All obtained products were calcined at different temperatures for 4 h.

2.2 Characterization Without any other treatments, fifty milligrams of the TiO_2 nanoparticles was dispersed in 10 ml of deionized water by ultrasonic treatment in an ultrasonic cleaning bath (Model KQ-250DE, 80 KHz, 100 W, China) for 30 min. Then, the suspension was transferred into 6 identical cuvettes. The dispersibility of TiO_2 nanoparticles was studied by the sedimentation method through a digital camera.

The phase constitution of the products was determined by powder X-ray diffraction (XRD) using a Bruker D8 Advance diffractometer. The average crystal size of anatase and rutile was also measured from the XRD patterns using the Scherrer equation. The morphology of the TiO_2 nanoparticles was investigated using a Hitachi H-600 transmission electron microscope (TEM). The surface adsorption properties of TiO_2 nanoparticles were characterized by fourier transformation infrared (FT-IR) spectra obtained with a Shimadzu FT-IR 8900 spectrometer. Thermo-gravimetric analysis (TGA) curves were obtained by a Mettler–Toledo (Switzerland) TGA 851e instrument with Ar as the buffer gas. The Zeta potentials (ζ) of TiO_2 nanoparticles were determined with Malvern, ZETASIZER 3000HSA. The specific surface areas of the nanoparticles were measured via the Brunauer–Emmett–Teller (BET) method with nitrogen absorption–desorption isotherms at –196 °C on a Micrometrics ASAP 2010 system. Pore diameter and pore volume were calculated using the Barrett–Joyner–Halenda (BJH) model.

3 Results and discussion As we know, nanoparticles have a strong tendency to grow into large particles in order to minimize the surface energy when the calcining temperature is increased. The large size leads to the increase of the sedimentation velocity and the decrease of the dispersibility of the particles [20, 21]. The TiO_2 nanoparticles that calcined at different temperature were re-dispers-

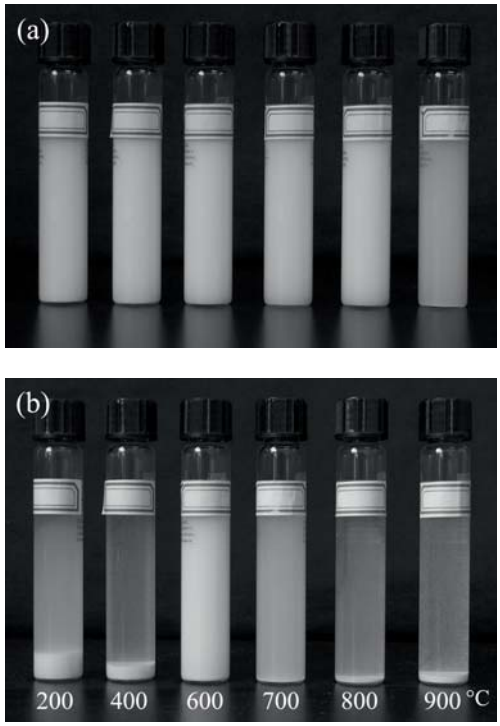

Figure 1 Photographs demonstrated the higher dispersibility of TiO_2 nanoparticles calcined at 600 °C and 700 °C, (a) taken immediately after dispersion; (b) taken after 6 h placement.

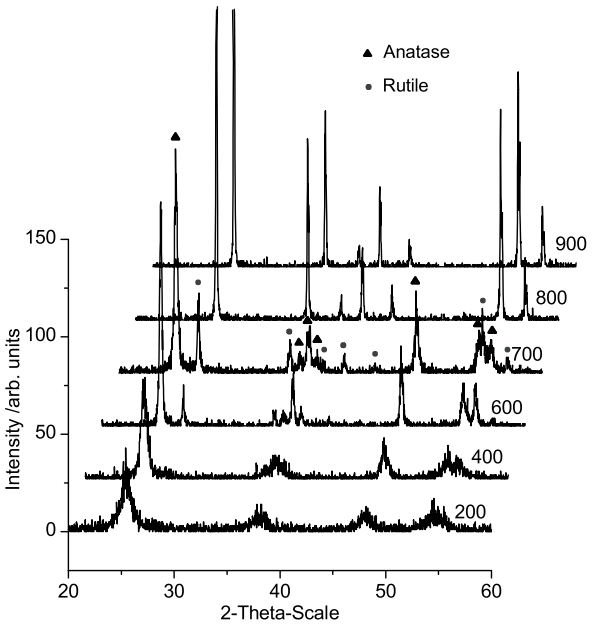

Figure 2 XRD patterns of the corresponding series of the TiO_2 in Fig. 1.

© 2009 WILEY-VCH Verlag GmbH & Co. KGaA, Weinheim

ed in water under same conditions (Fig. 1a). After they were settled for 6 h, the nanoparticles that calcined at 600 °C and 700 °C behaved abnormally, acting against the existing rule mentioned above. These two samples had the higher dispersibility than that of calcined at 400 °C (see Fig. 1b).

Figure 2 shows that the A–R phase transformation begins in the TiO_2 nanoparticles at about 600 °C, and the residual anatase phase still exists in the sample up to 700 °C. When the calcination temperature raises to 800 °C, the transformation from anatase to the rutile is complete. From the results mentioned in Figs. 1 and 2, it is deduced that the optimal dispersibility appears during the A–R phase transformation.

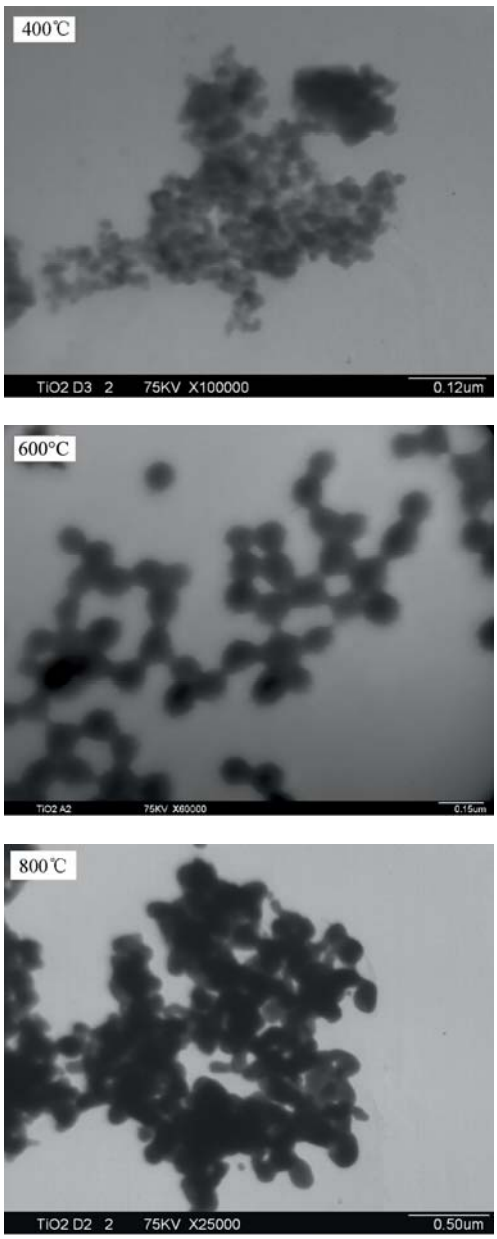

Figure 3 TEM images of TiO_2 nanoparticles calcined at the temperature of 400 °C, 600 °C and 800 °C, respectively.

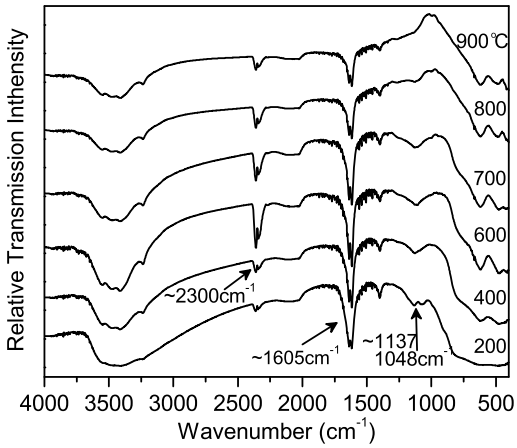

Figure 4 FT-IR spectra of samples filtered from corresponding dispersion system, and drying in vacuum at 50 °C for 1 h (10.0 mg sample was suspended in 1.0 g KBr crystal).

Figure 3 shows that the morphology of the TiO_2 nanoparticles are free-form at temperature under 400 °C, and the better crystallization spherical particles have come into being when the beginning of A–R phase transformation (600 °C). Although aggregation takes place at 800 °C, it is worthwhile to note that the surface morphology of the corresponding particles still maintains almost slippery sphericity. As mentioned earlier in the Refs. [22, 23], the A–R transformation could be initiated within the interface between two contacting anatase particles, and led to the formation of the better crystallization spherical particles.

Figures 4 and 5 show that there is an identifiable area augment of the bands at 1605 cm^{-1}, 1137 cm^{-1} and 1048 cm^{-1} for TiO_2 nanoparticles treated at 600 °C and 700 °C compared to others. A band at 1605 cm^{-1} is due to deformation vibrations of molecular water, which is an evidence of a large amount of water adsorbed onto TiO_2 surface in a molecular state. IR bands at 1137 cm^{-1} and 1048 cm^{-1} are attributed to the Ti–OH groups, which

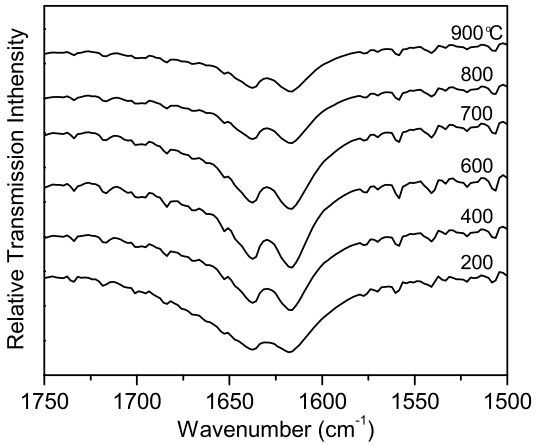

Figure 5 Enlarged FT-IR spectra of the samples calcined at 200–900 °C for the bands at 1605 cm^{-1}.

© 2009 WILEY-VCH Verlag GmbH & Co. KGaA, Weinheim

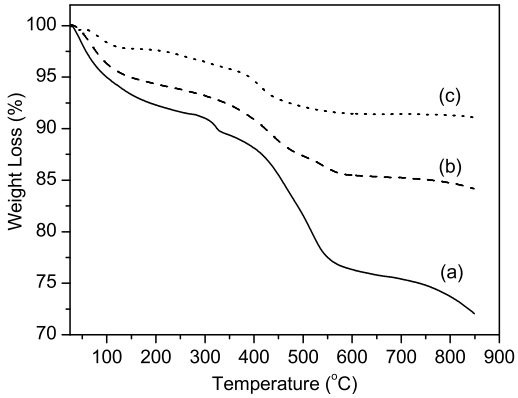

Figure 6 TGA curves for TiO_2 nanoparticles calcined at different temperatures of (a) 600 °C, (b) 400 °C, and (c) 800 °C, respectively.

formed stronger bonds with adsorbed water molecules [24, 25]. A peak at around 2300 cm^{-1} is ascribable to CO_2 adsorbed onto the TiO_2 surface [26], which also indicates that the surface of the TiO_2 calcined at 600 °C and 700 °C is favorable for the adsorption of molecular.

The hydration effect is also examined using TGA analysis. As shown in Fig. 6, the mass loss for three samples occurs in a wide temperature range from room temperature to 550 °C. The mass loss at temperatures lower than 100 °C indicates the presence of free water or physisorbed water, and that above 400 °C corresponds to the elimination of Ti–OH groups as water [25, 27]. Also, the water content for the sample calcined at 600 °C reaches as high as 15 wt%. The results revealed that the sample calcined at 600 °C had the most hydrated surface, compared to the other two samples.

Clearly, there is a noticeable difference among TiO_2 nanoparticles calcined at different temperature. Consequently, due to a high degree of curvature, the A–R transformation allows maintaining the higher density of hydrating water at the TiO_2 nanoparticles surfaces. The dispersive behaviors of TiO_2 nanoparticles in water medium will depend strongly on the water-induced repulsive interaction, which prevents from the aggregation of TiO_2 particles.

We know that the dispersion behaviors of nanoparticles depend not only on their increasing sizes and surface electrostatic properties, also on their steric hindrance effect. So the dispersion states of TiO_2 nanoparticles are affected by at two competitive interactions: (1) the interactions of van der Waals and electrostatic forces among TiO_2 particles, and (2) the interactions between TiO_2 particles and dispersion medium. Whereas, especially in water medium, a variety of experimental and theoretical studies given for the water adsorption on TiO_2 surfaces indicated that the hydration forces, which are highly relevant with the hydrogen bond interactions, are considered to be stronger than van der Waals forces and electrostatic repulsion [28–32].

Regarding the zeta potentials (ζ) and pH values of TiO_2 of corresponding dispersive systems, as presented in Table 1, we cannot observe a significant correlation between the surface charges of samples calcined at 600 °C or 700 °C and their dispersibility. Moreover, the corresponding pH values have a relatively little change. As expected, with increasing calcination temperature, the crystal size of all TiO_2 nanoparticles increases. These results confirm our ideas that surface charges and particle size are not crucial factors affecting the dispersibility of TiO_2 nanoparticles observed during A–R phases transformation.

Table 1 Zeta potentials and structural properties of TiO_2 nanoparticles calcined at different temperatures in water.

calcination temp. (°C)	200	400	600	700	800	900
ζ (mV)	31.6	15.4	5.0	–16.0	–33.3	–31.9
pH	3.52	3.51	3.61	4.11	4.15	4.35
size (nm)*	9.2	17.8	53.2	60.3	–	–
	–	–	47.7	64.5	187.7	220.8

* Anatase (upper row), rutile (lower row).

The thermal treatment of these particles leads to changes of BET surface area, pore volume and pore size distribution. The corresponding evolution of their structural properties is summarized in Table 2. With increasing calcination temperature from 600 °C to 700 °C, the BET surface areas of samples are interestingly high and stable without reduction of pore volume. This fact probably favored the relatively high structural stability of the obtained materials during A–R phases transformation.

Table 2 Summary of the physicochemical properties of TiO_2 powders.

calcination temp. (°C)	200	400	600	700	800	900
S_{BET} ($m^2\ g^{-1}$)	239.5	206.4	156.1	142.6	50.5	8.9
central pore size (nm)	2.7	3.2	3.7	4.0	9.8	10.2
total volume ($cm^3\ g^{-1}$)	0.25	0.19	0.18	0.18	0.10	0.02

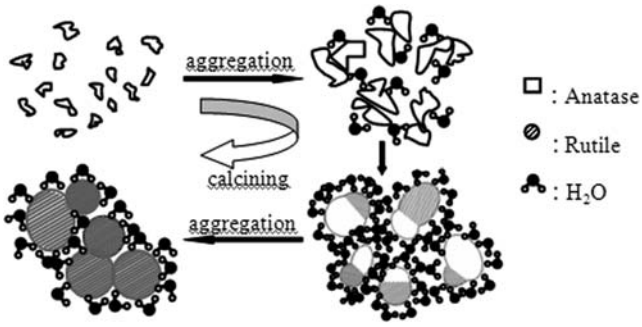

Figure 7 Visual model illustrated the spherical particles of TiO_2 allowed maintaining the high density of hydrating water on the surface of TiO_2 nanoparticles during phase transformation from A–R.

© 2009 WILEY-VCH Verlag GmbH & Co. KGaA, Weinheim

All existing data we obtained suggest that A–R transformation allows maintaining the higher density of hydrating water on the TiO_2 nanoparticles surfaces, which induces stronger repulsive interaction and prevents TiO_2 particles from aggregating. The visual model was presented in the Fig. 7.

4 Conclusions In this paper, we present the observation of the highly stable dispersibility during A–R phase transformation in the TiO_2 nanoparticles. XRD, TEM and FT-IR measurements show that the phase transformation leads to the formation of the better crystallization spherical particlesis, which are in favour of water being adsorbed onto the surface of the TiO_2 nanoparticles. This surface repulsive hydration forces that impede particles aggregation result in the highly stable dispersibility of TiO_2 nanoparticles in water medium. Regarding the zeta potentials (ζ) and the crystal size of TiO_2 of corresponding dispersive systems, we can not observer the significant correlation between the surface charges and the crystal size of samples calcined at 600 °C or 700 °C and their dispersibility. Thus, it can be deduced that the surface electrostatic forces and interactions of van der Waals among TiO_2 particles are not crucial factors in the highly stable dispersibility of TiO_2 observed during A–R phases transformation. However, further investigations have to be carried out to understand the dispersive mechanism more detailedly.

Acknowledgements The authors greatly thank Professor Yunchang Fan for advice to our paper. This work was financially supported by the National Natural Science Foundation of China (Grant No. 20671028) and the Graduate Student Scientific Research Foundation of Hebei Normal University (No. 200801008).

References

[1] M. R. Hoffmann, S. T. Martin, W. Choi, and D. W. Bahnemann, Chem. Rev. **95**, 69–96 (1995).
[2] X. Z. Li, H. Liu, L. F. Cheng, and H. J. Tong, Environ. Sci. Technol. **37**, 3989–3994 (2003).
[3] M. Adachi, Y. Murata, J. Takao, J. T. Jiu, M. Sakamoto, and F. M. Wang, J. Am. Chem. Soc. **126**, 14943–14949 (2004).
[4] K. Zakrzewska, Thin Solid Films **391**, 229–238 (2001).
[5] K. Kalyanasundaram and M. Grätzel, Coord. Chem. Rev. **177**, 347–414 (1998).
[6] S. Yin, Y. Inoue, S. Uchida, Y. Fujishiro, and T. Sato, J. Mater. Res. **13**, 844–847 (1998).
[7] T. Ohno, K. Sarukawa, K. Tokieda, and M. Matsumura, J. Catal. **203**, 82–86 (2001).
[8] J. Yu, J. C. Yu, W. Ho, and Z. Jiang, New J. Chem. **26**, 607–663 (2002).
[9] B. Sun and P. G. Smirniotis, Catal. Today **88**, 49–59 (2003).
[10] O. Carp, C. L. Huisman, and A. Reller, Prog. Solid State Chem. **32**, 33–177 (2004).
[11] Y. Shu, H. Hitoshi, M. Daisaku, I. Masayuki, and S. Tsugio, J. Photochem. Photobiol. A **163**, 1–8 (2004).
[12] A. Fujishima, T. N. Rao, and D. A. Tryk, J. Photochem. Photobiol. C **1**, 1–21 (2000).
[13] Q. H. Zhang, L. Gao, and J. K. Guo, Appl. Catal. B **26**, 207–215 (2000).
[14] R. R. Bacsa and J. Kiwi, Appl. Catal. B **16**, 19–29 (1998).
[15] J. C. Yu, J. G. Yu, W. K. Ho, and L. Z. Zhang, Chem. Commun., 1942–1943 (2001).
[16] S. Bakardjieva, J. Šubrt, V. Štengl, M. J. Dianez, and M. J. Sayagues, Appl. Catal. B **58**, 193–202 (2005).
[17] J. Ovenstone, J. Mater. Sci. **36**, 1325–1329 (2001).
[18] Y. Hu, H. L. Tsai, and C. L. Huang, J. Eur. Ceram. Soc. **23**, 691–696 (2003).
[19] L. Miao, S. Tanemura, Y. Kondo, M. Iwata, S. Toh, and K. Kaneko, Appl. Surf. Sci. **238**, 125–131 (2004).
[20] M. S. Selim, A. C. Kothari, and R. M. Turian, AIChE J. **29**, 1029–1038 (1983).
[21] R. Buscall, J. W. Goodwin, R. H. Ottewill, and Th. F. Tadros, J. Colloid Interface Sci. **85**, 78–86 (1982).
[22] H. Zhang and J. F. Banfield, Am. Mineral. **84**, 528–535 (1999).
[23] R. L. Penn and J. F. Banfield, Geochim. Cosmochim. Acta **63**, 1549–1557 (1999).
[24] M. A. Henderson, Surf. Sci. **355**, 151–166 (1996).
[25] T. Bezrodna, G. Puchkovska, V. Shymanovska, J. Baran, and H. Ratajczak, J. Mol. Struct. **700**, 175–181 (2004).
[26] K. Nagaveni, M. S. Hegde, N. Ravishankar, G. N. Subbanna, and G. Madras, Langmuir **20**, 2900–2907 (2004).
[27] N. Nakayama and T. Hayashi, Colloids Surf. A **317**, 543–550 (2008).
[28] U. Diebold, Surf. Sci. Rep. **48**, 53–229 (2003).
[29] G. S. Li, L. P. Li, J. B. Goates, and B. F. Woodfield, J. Am. Chem. Soc. **127**, 8659–8666 (2005).
[30] A. P. Kulkarni and D. S. Muggli, Appl. Catal. A **320**, 274–282 (2006).
[31] G. W. Lee and S. Kumar, J. Phys. Chem. B **109**, 17128–17133 (2005).
[32] H. T. Ham, Y. S. Choi, and I. J. Chung, J. Colloid Interface Sci. **286**, 216–223 (2005).

© 2009 WILEY-VCH Verlag GmbH & Co. KGaA, Weinheim